Investigation of dynamic behavior of auxiliary power unit with rotor in gas foil bearings

Joury Temis, Mikhail Temis, Andrey Egorov, Valentin Gavrilov

Investigation of dynamic behavior of auxiliary power unit with rotor in gas foil bearings

Joury Temis[1,2*], Mikhail Temis[1,2], Andrey Egorov[1], Valentin Gavrilov[1]

ISROMAC 2016

International Symposium on Transport Phenomena and Dynamics of Rotating Machinery

Hawaii, Honolulu

April 10-15, 2016

Abstract

Auxiliary power unit rotor static and dynamic characteristics were investigated for four rotor supporting schemes. Auxiliary power unit rotor supported in roller element bearings was compared to similar rotor supported in gas foil bearings and to intermediate option of rotor supported in combination of gas foil bearing and ball bearing. Support reactions under the action of weight, imbalance and flight acceleration forces are determined for all schemes. Rotor support reactions gives an opportunity to select gas foil bearing type and dimensions.

Rotor model for nonlinear analysis is based on beam finite elements and verificated with corresponding solid model by comparison of eigenfrequencies. This model taking into account supports casing stiffness characteristics determined using 3D finite-element models and nonlinear stiffness properties of roller element and/or gas foil bearings. Different schemes of rotor supporting are analyzed for support loads, eigenfrequencies and nonlinear vibration orbits and amplitudes that allows selecting major problems for upgrading of auxiliary power unit rotor with gas foil bearings.

Keywords

Oil-free engine — gas foil bearing — rotordynamics

[1] *Central Institute of Aviation Motors, Moscow, Russia*

[2] *Bauman Moscow State Technological University, Moscow, Russia*

*__Corresponding author__: tejoum@ciam.ru

INTRODUCTION

From one side application of gas foil bearings in supports of small gas turbine engines rotor allows in perspective to create a “dry” engine and changes limits of rotor rotational frequency. That sufficiently influences on engine structure, mass characteristics, reliability, cost of manufacturing and operation [1]. However, from another side application of gas foil bearings in rotor supports requires solution of a number of problems such as creating of sufficient carrying force, response on non-stationary loads, reliability at high temperatures etc. Most of these problems solved using different foils structure. Regardless all peculiarity of gas foil bearings at present time they find increasingly greater application in supports of small gas turbine engines [2].

There are large amount of works devoted to rotor in gas foil bearings operational characteristics investigation. The major part of them using experimental methods for rotor in gas foil bearings dynamics investigation as it presented in [3, 4]. However there are a number of works where numerical and experimental approaches are using together [5, 6]. Apart of them paper regarding to numerical [7] and experimental [8, 9] investigation of individual gas foil bearings that allows to investigate bearing characteristics for different elastic foils structure simulating various operational conditions.

Traditional schemes of high-speed auxiliary power unit rotor are well known. However, operation of specific engine is different from other due to a big number of stiffness and damping rotor-bearing-casing system parameters. Therefore, the aim of replacing of rolling element bearings with gas foil bearings for rotor of existing auxiliary power unit requires at first stage an investigation of engine parameters and it sensitivity to their changing.

Basing on mathematical models developed by authors [10-12] an investigation of dynamic behavior of auxiliary power unit supported in gas foil bearings or roller element bearings is carried out in present paper.

1. ENGINE CHARACTERISTICS

Auxiliary power unit used for investigation in current paper have a rotor scheme as presented in fig. 1 (Scheme 1). Rotor weight is about 3.5 kg and nominal rotating frequency 38 500 rpm. Engine have a one rotor with mounted one stage centrifugal compressor and one stage axial turbine. In initial configuration rotor is supported in one ball bearing in front support and one roller bearing in back support. So front support carry both part of radial load and full axial load.

All supports should use gas bearings in final upgraded rotor configuration. Proposed support designs should not change engine structure sufficiently. However, ordinary gas journal bearings have greater length then roller element bearings in existing engine. Besides this after changing of ball bearing with radial gas bearing, the thrust gas bearing should be installed for compensation of axial force. Thrust bearing also needs a sufficient radial space for a runner.

Engine structure allows several schemes for using gas bearings in rotor supports. Usually radial and thrust gas

bearings located between compressor and turbine. However, due to limited distance between compressor and turbine in existing engine there is small base length between centers of radial supports in such scheme (fig. 1, Scheme 4). So for increasing lateral stability of the rotor the supplementary part was installed at the back where radial and thrust gas bearings was mounted (fig. 1, Scheme 3). Also intermediate rotor scheme with one ball bearing in front support and one radial gas bearing mounted on supplementary rotor part as rotor back support (Scheme 2) is presented in fig. 1b. This scheme allows only to change bearing type in hot part of engine.

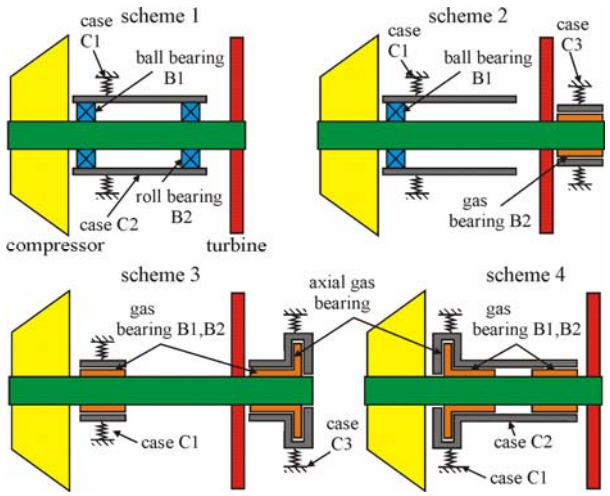

Figure 1. Power unit rotor schemes

Comparison of presented supporting schemes eigenfrequencies, radial loads distribution and orbits during startup and operation conditions allows to show advantages of each scheme.

2. ROTOR MODELS

Rotor finite element solid models corresponding to each rotor supporting scheme as presented in fig. 1 are developed for investigation (fig. 2). Rotor was simulated by 20-node finite elements, compressor and turbine blades simulated as disks with corresponding density and stiffness. For all tighten rotor elements contact on faces was simulated as bonded.

These models are used for calculation of supports reactions and stress-strain state under the action of gravity and operational loads. Results for support reactions in all schemes presented in table 1 for four load cases. In load case I rotor is fixed and only weight force (g) is acting. In load case II rotor rotating at maximum operating frequency and weight force and imbalance inertia force (me) are acting. For load cases III and IV, besides rotor imbalance inertia force the acceleration during airplane horizontal (2g) and vertical (4g) evolution is taken into account. Reactions values in table 1 give information of maximum support loads at startup and operation for further selection of gas foil bearing dimensions and structure. Gas bearings should provide rotor floating-up at startup and compensation of operational loads. According to presented results radial gas foil bearing should be designed for radial load at startup for load about 30 N and at evolutions in operational conditions for load up to 150 N.

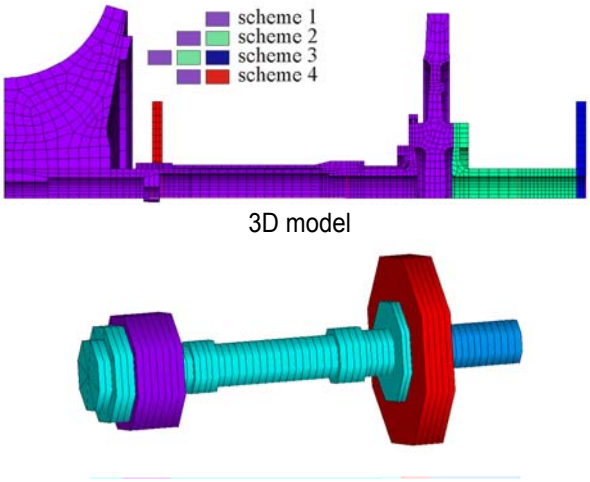

3D model

Bernoulli beam model

Figure 2. FE model of rotor

Table 1. Reactions in rotor supports

	Scheme 1	Scheme 2	Scheme 3	Scheme 4
Rotor mass, kg	3,63	3,99	4,28	3,93
Reaction forces in B1, N				
I (g	13,87	24,71	23,56	22,72
II (g+me)	22,87	33,71	32,55	32,9
III(2g+me)	35,96	59,82	57,27	56,1
IV(4g+me)	78,37	132,55	126,78	123,76
Reaction forces in B2, N				
I (g	22,42	15,21	19,27	16,59
II (g+me)	31,42	24,21	28,28	24,4
III(2g+me)	54,75	38,88	47,8	41,19
IV(4g+me)	121,1	85	105,4	90,77

Support finite element used in rotor model taking into account bearing stiffness and support casing stiffness. Bearing stiffness determined by special models depending upon bearing type and structure. Casing stiffness in bearing position determined by finite element model (fig. 3). Casing stiffness C1 (in plane section of support B1): $K_u = 7.5 \cdot 10^7$ N/m, $K_{Rot\_u} = 2.07 \cdot 10^4$ N·m/rad. Casing stiffness C2 (cylindrical casing between supports B1 and B2): $K_u = 5.2 \cdot 10^7$ N/m, $K_{Rot\_u} = 3.6 \cdot 10^5$ N·m/rad. Stiffness of casing C3 is $K_u = 5 \cdot 10^9$ N/m.

In rotor dynamic analysis, the beam rotor models are used. For improvement of beam models in simulation of stiffness characteristics for complex geometry rotor details the special finite elements with general 6x6 matrix are used. Such general matrix is calculated using detail 3D models of rotor

elements. There are gratifying correspondence between results for all models after verification of beam model versus 3D model, (table 2).

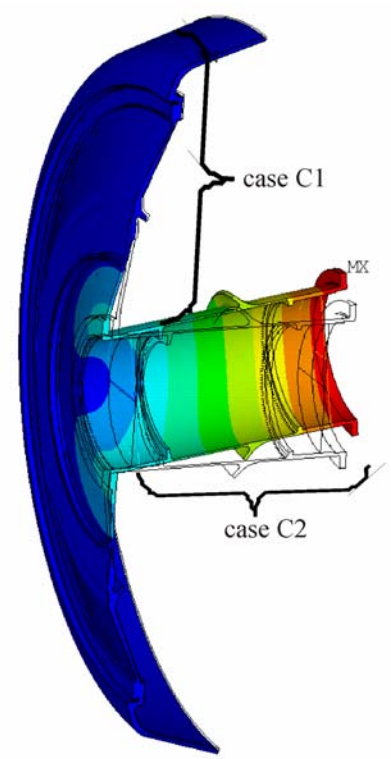

Figure 3. Casing FE model and deformed geometry

Table 2. Rotor beam model verification

	№	Eigenvalue, rpm		δ, %
		Solid model	Beam model	
Scheme 1	1	6055	6109	0,89
	2	35905	32675	-9
Scheme 2	1	7535	7571	0,48
	2	35338	32185	-8,9
Scheme 3	1	7974	7609	-4,6
	2	8073	8078	0,1
Scheme 4	1	4943	4671	-5,5
	2	7093	7241	2,1

3. GAS BEARINGS SELECTION

The gas foil bearings with one top foil and bump foil are selected for current investigation (fig. 4a). Mathematical models for presented bearing for different shaft journal diameters and bearing length are created. Gas foil bearings carrying force and attitude angle calculated on the base of bearing mathematical model developed in [10]. This model is used nonlinear Reynolds equation for compressible fluid for calculation of gas flow in bearing. The step process for shaft eccentricity in bearing with self-correcting procedure [13] at each step is used for solution of nonlinear Reynolds equation. For determination of top foil radial deflections the 2D contact interaction model between top foil, bump foil and bearing race are created (fig. 4a). This model includes elastic Coulomb friction model and provides an actual bump foil circumferential displacement. Contact interaction model taking into account friction interaction between bearing top foil and bump foil, bump foil and bearing race with friction coefficient depending on foils and bearing race material and coating. Friction coefficient varying in range between 0.1 and 0.3 in current models. Discrete contact interaction of top and bump foils allows to simulate top foil deformations between bumps. Carrying out calculations for shaft journal diameters and bearing length in range of values that conforms to major engine dimensions allows to determine bearing diameter and length array satisfying by carrying force for support reaction values in table 1.

Bearing diameter of 30 mm equal to rotor diameter in support area is chosen from this array. Radial gas foil bearing parameters is presented in table 3.

Table 3. Foil bearing parameters

Bearing diameter D1, mm	30
Length, mm	42
Number of top foils	1
Bump foil thickness, mm	0.1
Top foil thickness, mm	0.1

Bearing carrying force and attitude angle presented in fig. 5 and 6 for rotor rotating frequency of 5000 rpm and support temperature of 20°C and 400°C correspondingly. Bearing characteristics are represented in terms of the dimensionless eccentricity ratio $\chi = e/\delta$, where e is a shaft journal eccentricity and δ is a radial clearance in bearing.

Table 4. Rolling and gas foil bearing (T = 20°C) linearized stiffness

№	Rotating frequency, rpm	Stiffness, N/m	
		B1	B2
Scheme1	all	$2 \cdot 10^8$	$3 \cdot 10^8$
Scheme 2	5000	$2 \cdot 10^8$	$1.02 \cdot 10^6$
	20000		$5 \cdot 10^6$
	42000		$8.65 \cdot 10^6$
Scheme 3	5000	$1.74 \cdot 10^6$	$1.31 \cdot 10^6$
	20000	$5.36 \cdot 10^6$	$5.19 \cdot 10^6$
	42000	$9.31 \cdot 10^6$	$8.98 \cdot 10^6$
Scheme 4	5000	$1.64 \cdot 10^6$	$1.135 \cdot 10^6$
	20000	$5.33 \cdot 10^6$	$5.07 \cdot 10^6$
	42000	$9.25 \cdot 10^6$	$8.76 \cdot 10^6$

According to operating parameters of engine, there is an axial force need to be compensated by thrust foil bearing. Thrust bearing characteristics selected on the analogy of the data presented in [14]. Using in investigation gas foil bearings 3D solid models presented in fig. 4b and 4c for different rotor supporting schemes. For Scheme 1 and Scheme 2 the rolling

element bearings stiffness need to be determined for support finite element considering bearings nonlinear characteristics. This was done using Hertz contact theory [15]. Calculated bearing stiffness are $K_1 = 2 \cdot 10^8$ N/m (B1) and $K_2 = 3 \cdot 10^8$ N/m (B2).

Gas foil bearing linearized stiffness values corresponded to shaft equilibrium position in bearing in operation regime are presented for a number of rotating frequencies in table 4.

Angular stiffness for thrust bearing is $K_{Rot\_u} = 4.9 \cdot 10^3$ N·m/rad (Schemes 3-4).

4. ROTOR EIGENFREQUENCIES ESTIMATION

Rotor supports stiffness sufficiently changes from Scheme 1 to others due to replacing of rolling element bearings with gas bearings and changing of support location. For engine in gas bearings operating capacity it eigenfrequencies, eigenmodes and critical speeds for each supporting scheme should be determined and correlated with range of rotor rotating frequencies. Engine maximum operating speed is 42000 rpm. Rotor finite element solid models (fig. 2) that taking into account rotor gyroscopic moments are used for calculation. Eigenmodes, eigenfrequencies and Campbell diagrams for four rotor supporting schemes are presented in fig. 7.

Replacing of roller element bearings with gas foil bearings brings to sufficiently decreasing of supports stiffness. Besides this in Scheme 2 and Scheme 3 distance between supports B1 and B2 is increased. Casing of support B2 have greater stiffness regards to individual connection to engine casing in Scheme 2 and Scheme 3 instead of console connection (fig. 1) for Scheme 1 and Scheme 4.

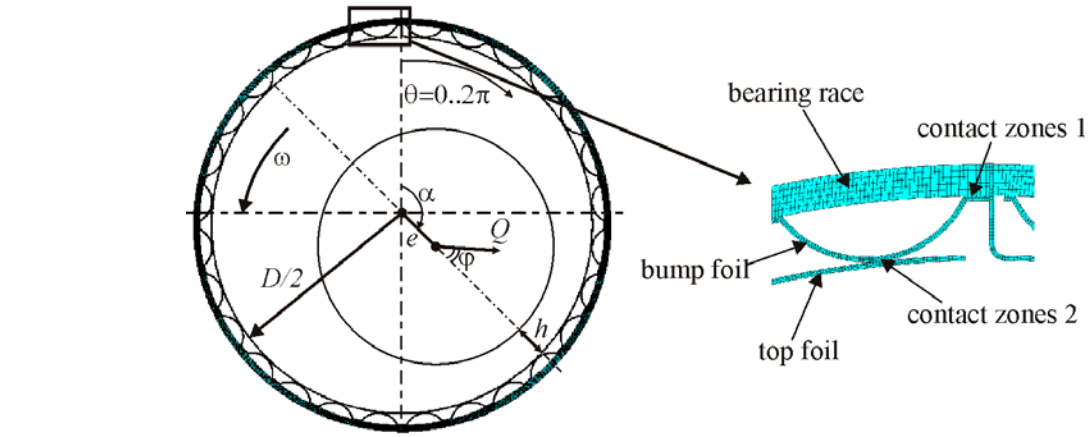

a) radial foil bearing scheme and finite-element model

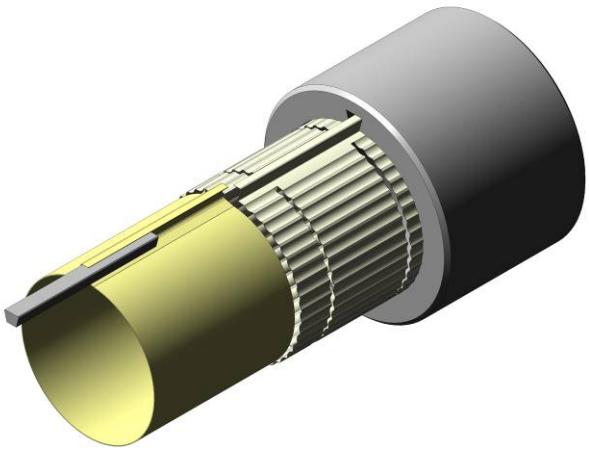

b) radial bearing solid model

c) thrust bearing solid model

Figure 4. Gas foil bearings

Critical speeds for forward precession represented in table 5 for all schemes. Rotor for all four schemes have one similar eigenmode: angular vibrations of rotor as rigid body due to casing angular small stiffness. This mode corresponds to first critical speed f_1 for Scheme 1 and Scheme 4. It is decreased for Scheme 4 in comparison with Scheme 1 on 15% by decreasing of radial support stiffness. Angular vibrations of rotor as rigid body also corresponds to first critical speed f_1 for Scheme 2 and for second critical speed f_2 for Scheme 3 and it is increased on 64% for Scheme 2 and on 72% for Scheme 3 in comparison with Scheme 1 first critical speed value (f_1). Increasing of corresponding critical

speed for Scheme 2 explained by increasing distance between supports B1, B2 and individual support for B2. Besides this in Scheme 3, the thrust bearing was installed and this explain critical speed growth in comparison with Scheme 2.

Another mode for Scheme 1 and Scheme 2 is a lateral rotor bending vibrations in supports. Corresponding critical speed for Scheme 1 (f_2) and Scheme 2 (f_2) have close values. Influence of rotor supports location and B2 support stiffness change appears by slight decreasing of critical speed for Scheme 2.

Another mode for Scheme 3 (f_1) and Scheme 4 (f_1) is a lateral rotor vibration as rigid body in gas foil supports. It have less value of critical speed for Scheme 4 because of location of B1 and B2 supports on same console (fig. 1).

All eigenfrequencies values are increasing with rotating frequency growing due to gyroscopic moments (all schemes) and increasing of gasdynamic stiffness (schemes 2-4). The gyroscopic moment influence on eigenmode value is sufficient for eigenmodes where rotor angular displacement is dominant (Scheme 3 - f_2, Scheme 4 - f_1).

For all schemes rotor passing through first critical speed at running up in range of rotating frequencies 7500-11500 rpm. For Scheme 1 second rotor critical speed is equal to 40500 rpm and greater then rotor maximum operational speed. For Scheme 2 the second rotor critical speed (39000 rpm) dropped almost until maximum operation speed. First and second critical speeds for schemes 3 and 4 are close to each other and lie in range of frequencies 7500-11500 rpm. There is a big region for Scheme 2 and Scheme 3 where eigenfrequencies are close to rotor frequency.

Table 5. Critical speed

№	Critical speed (forward precession), rpm	
	f_1	f_2
Scheme1	6700	40500
Scheme 2	11000	39000
Scheme 3	9000	11500
Scheme 4	5700	7500

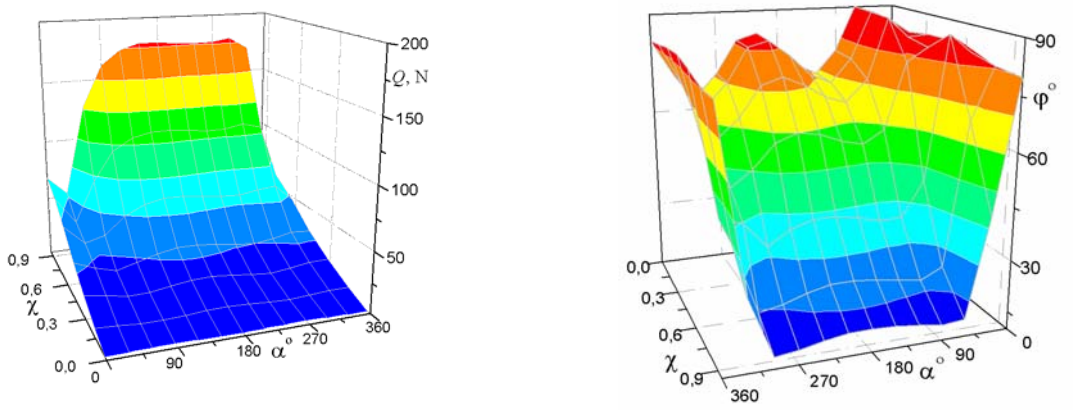

a) carrying force b) attitude angle

Figure 5. Gas bearing characteristics (T = 20°C)

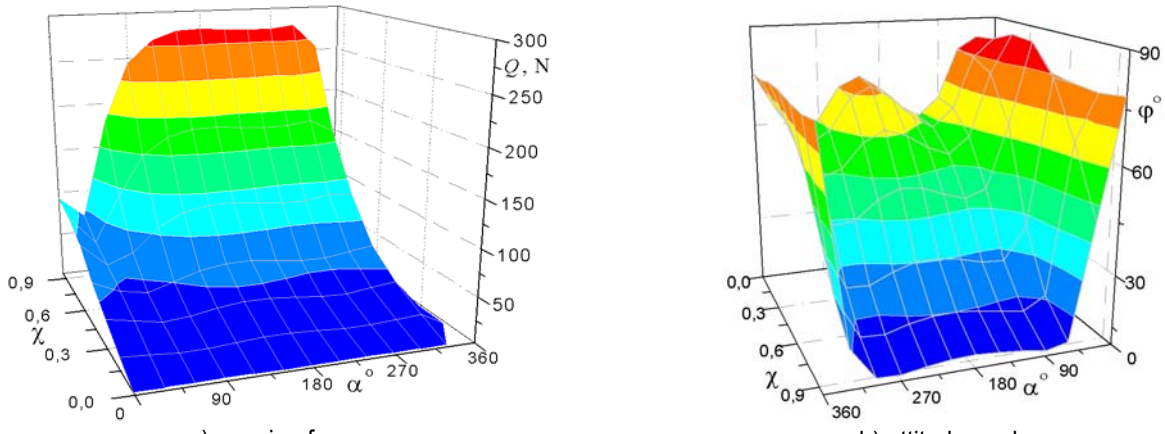

a) carrying force b) attitude angle

Figure 6. Gas bearing characteristics (T = 400°C)

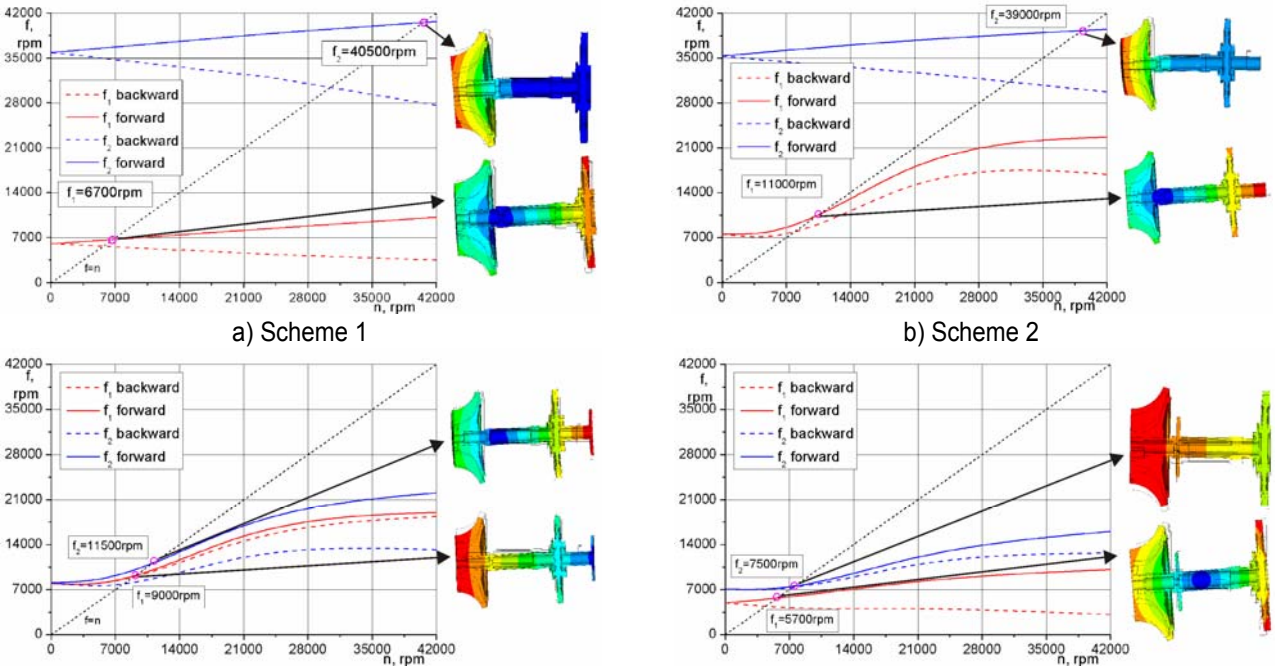

a) Scheme 1 b) Scheme 2

c) Scheme 3 d) Scheme 4

Figure 7. Campbell diagrams and eigenmodes for different rotor supporting schemes

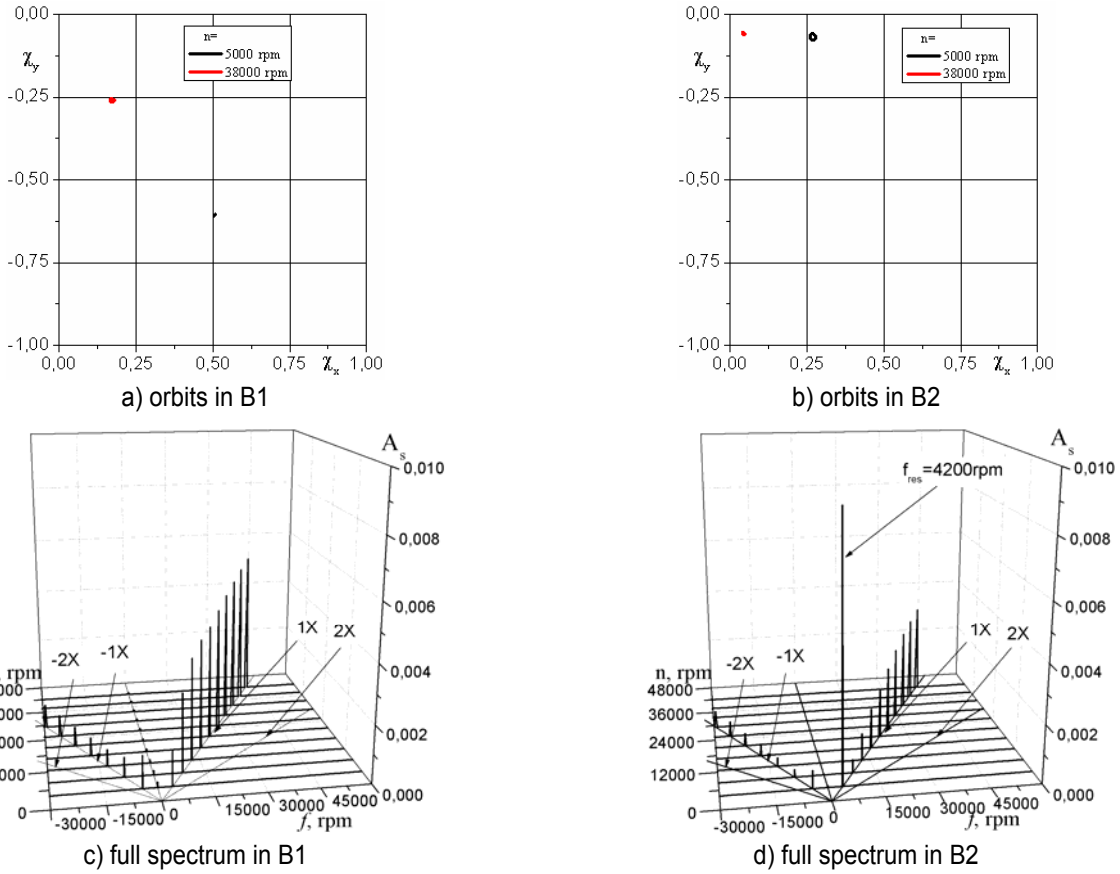

a) orbits in B1 b) orbits in B2

c) full spectrum in B1 d) full spectrum in B2

Figure 8. Scheme 4: structural damping 0.003, T = 20°C

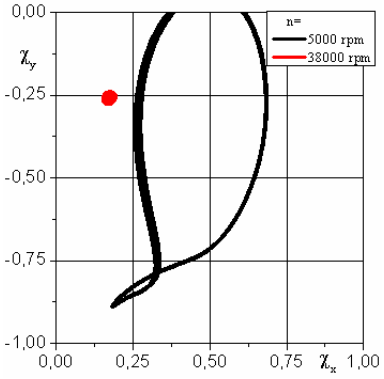

a) orbits in B1

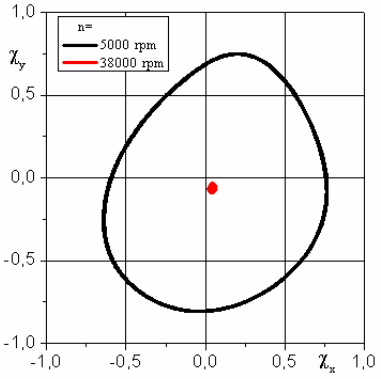

b) orbits in B2

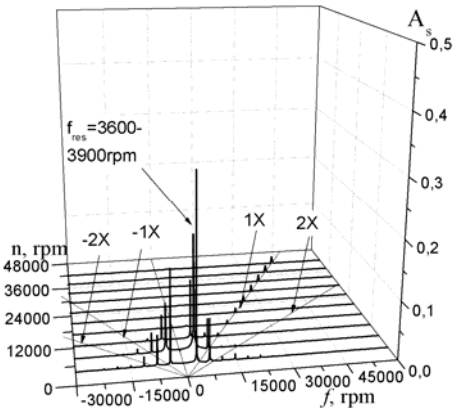

c) full spectrum in B1

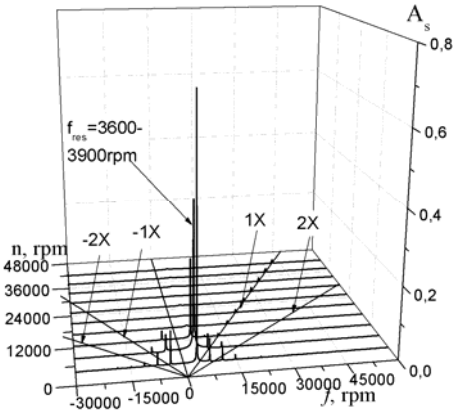

d) full spectrum in B2

Figure 9. Scheme 4: structural damping 0.001, T = 20°C

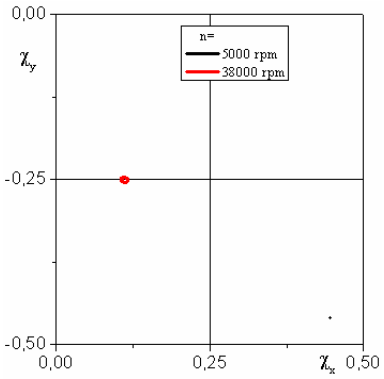

a) orbits in B1

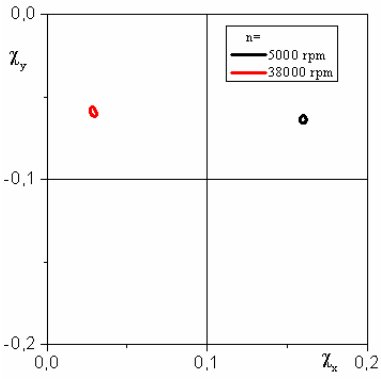

b) orbits in B2

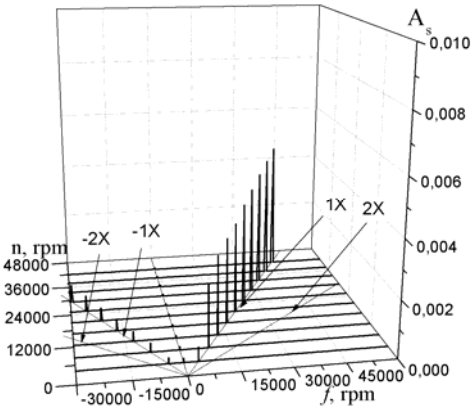

c) full spectrum in B1

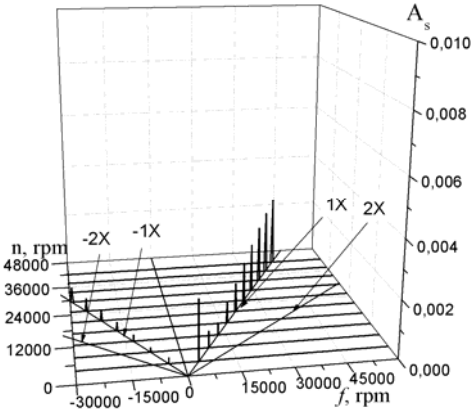

d) full spectrum in B2

Figure 10. Scheme 4: structural damping 0.003, T = 400°C

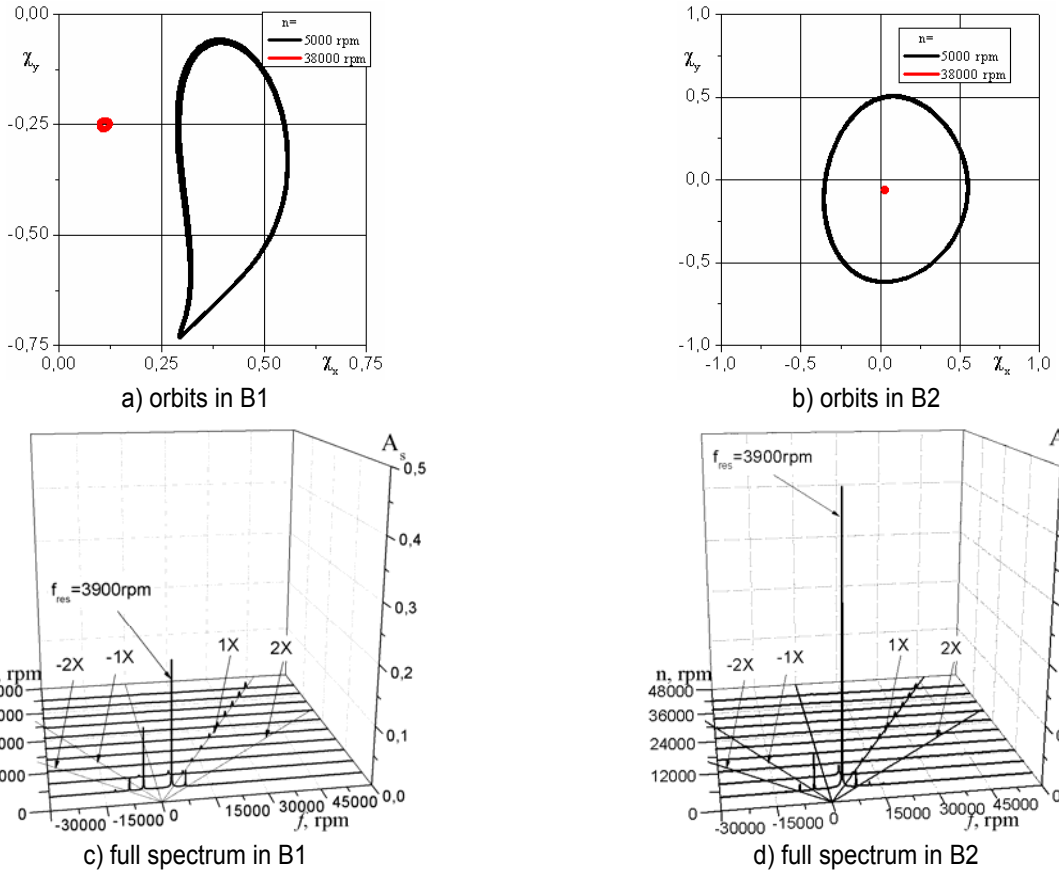

a) orbits in B1

b) orbits in B2

c) full spectrum in B1

d) full spectrum in B2

Figure 11. Scheme 4: structural damping 0.001, T = 400°C

5. ROTOR DYNAMIC BEHAVIOR INVESTIGATION

On fourth stage, the rotor dynamic behavior in whole range of rotating frequencies was investigated and rotor orbits in bearing were determined (fig. 8-11). Gas foil bearings under the action of dynamic radial loads caused by rotor imbalance and non-stationary loads was investigated. In each support the imbalance force of 1 g·mm is applied and normal gravity force acting on all rotor model. For direct integration of rotor nonlinear equations the Newmark scheme (δ = 1/2 and α = 1/4) with iterative refinement regarding to bearing carrying force is implemented.

As demonstrated in fig. 9 and 11 the simulation of rotor in gas foil bearings dynamics allows occurrence of subharmonic vibrations for small structural damping in system. These vibrations started when rotor speed approaches to first critical speed and lasting in some range. This range is shorter for hot supports conditions. Rotor orbits in both supports have elliptical or even more extended shape in this range. Rotor vibrations corresponds to first mode and have a big magnitude. When increasing rotor rotation frequency the rotor rotates on stable regimes around equilibrium position with small amplitude.

Stable regimes of rotor rotation are received in rotor dynamics simulation for structural damping of 0.003. All rotor orbits for both cold and hot conditions are circular and amplitudes are small (fig. 8 and 10).

6. CONCLUSION

An opportunity of auxiliary power unit design changing for implementation of gas foil bearing in rotor supports is shown. Bearing parameters including dimensions, geometry etc. for providing required carrying force are determined. Several schemes of rotor supports replacing with gas foil bearings are proposed. Analysis of support loads in operational and overload regimes as well as eigenvalue analysis and dynamic analysis shows working capacity of rotor supported in gas foil bearings. All presented schemes involves small modification of exist engine structure and this limiting the changes need to be performed for replacing of roller type bearings with gas foil bearings.

REFERENCES

[1] H. Heshmat. Advancement in the Performance of Aerodynamic Foil Journal Bearings- High Speed and Load Capacity. *ASME Journal of Tribology*, 116, pp. 287-95, 1994.

[2] C. DellaCorte, R.J. Bruckner. Remaining Technical Challenges and Future Plans for Oil-free Turbomachinery. In: *ASME Turbo Expo 2010: Power for Land, Sea and Air*, Glasgow, UK: p. 10, 2010.

[3] D. Rubio, L. San Andres. Bump-type foil bearing structural

stiffness: experiments and predictions. Proceedings of ASME Turbo Expo 2004*: Power for Land, Sea and Air*, Vienna, Austria: GT2004-53611

[4] T. Ho Kim, J. Lee, C. Ho Kim, Y. Lee. Rotordynamic performance of an oil-free turbocharger supported on gas foil bearings: effects of an assembly radial clearance. Proceedings of ASME Turbo Expo 2010*: Power for Land, Sea and Air*, Glasgow, UK: GT2010-23243.

[5] J. F. Walton II, H. Heshmat. On the coupling of foil bearing supported rotors: part 1 – analysis. Proceedings of ASME Turbo Expo 2007*: Power for Land, Sea and Air*, Montreal, Canada: GT2007-27821

[6] M. J. Tomaszewski, J. F. Walton II, H. Heshmat. On the coupling of foil bearing supported rotors: part 2 – experiment. Proceedings of ASME Turbo Expo 2007*: Power for Land, Sea and Air*, Montreal, Canada: GT2007-27825

[7] S. Le Lez, M. Arghir, J. Frene. A new bump-type foil bearing structure analytical model. Proceedings of ASME Turbo Expo 2007*: Power for Land, Sea and Air*, Montreal, Canada: GT2007-27078

[8] L. San Andres, D. Rubio, T. Ho Kim. Rotordynamic performance of a rotor supported on bump type foil gas bearings; experiments and predictions. Proceedings of ASME Turbo Expo 2006*: Power for Land, Sea and Air*, Barcelona, Spain: GT2006-91238

[9] M. Salehi, H. Heshmat, J.F. Walton II. Advancements in the structural stiffness and damping of a large compliant foil journal bearing: an experimental study. Proceedings of ASME Turbo Expo 2004*: Power for Land, Sea and Air*, Vienna, Austria: GT2004-53860

[10] J.M. Temis, M.J. Temis, A.B. Meshcheryakov. Gas-dynamic foil bearing model. *J. of Friction and Wear*. Vol. 32, № 3: 212-220, 2011.

[11] J.M. Temis, M.J. Temis, A.M. Egorov, A.B. Mescheryakov: Dynamics of compact gas turbine rotor supported by gas bearing. In: 8th IFToMM International Conference on Rotordynamics. KIST, Seoul, Korea, 2010.

[12] J.M. Temis, M.J. Temis, A.M. Egorov, V.V Gavrilov. Numerical and Experimental Investigation of Rotor-simulator in Foil Gasdynamic Bearings for Compact Gas Turbine. In: 9th IFToMM International Conference on Rotordynamics. Milan, Italy, 2014.

[13] J.M. Temis. Selfcorrection Step by Step Method for Solution of Nonlinear Elasticity and Plasticity Problems. CIAM Proceedings, № 918, 24 p., 1980 (in Russian).

[14] A.M. Gad, S. Kaneko. Performance characteristics of gas-lubricated bump-type foil thrust bearing. In: *Proceedings of the Institution of Mechanical Engineers, Part J: Journal of Engineering Tribology,* June 2015, vol. 229, 6: pp. 746-762.

[15] Rolling element bearings. Calculation, design and service of supports / Edited by L.Ya. Perelya and A.A. Filatov. Reference book, Moscow, Mashinostroenie, 543 p., 1992.